The discrete fractional Fourier transform based on the DFT matrix

Ahmet Serbes *, Lutfiye Durak-Ata

Yildiz Technical University, Department of Electronics and Communications Engineering, Yildiz, Besiktas, 34349 Istanbul, Turkey

A R T I C L E   I N F O

A B S T R A C T

We introduce a new discrete fractional Fourier transform (DFrFT) based on *only* the DFT matrix and its powers. Eigenvectors of the DFT matrix are obtained in a simple-yet-elegant and straightforward manner. We show that this DFrFT definition based on the eigentransforms of the DFT matrix mimics the properties of continuous fractional Fourier transform (FrFT) by approximating the samples of the continuous FrFT. By appropriately combining existing commuting matrices we obtain a new commuting matrix which performs better. We show the validity of the proposed algorithms by computer simulations comparing DFrFT points and continuous FrFT samples for various signals.

© 2010 Elsevier B.V. All rights reserved.

1. Introduction

The fractional Fourier transform (FrFT) has been popular in signal processing [1], time–frequency analysis [2,3], filter design [4], signal compression [5], parameter estimation [6,7], and pattern recognition [8]. As it is a powerful tool in signal processing, a discrete definition of FrFT which inherits the properties of its continuous counterpart is of much interest in recent years. Santhanam et al. [9] defined a discrete fractional Fourier transform (DFrFT) by using Taylor series expansion of the DFT matrix followed by the application of Cayley–Hamilton theorem and defined DFrFT as a weighted sum of its powers. However the definition fails to approximate the samples of the continuous FrFT, because the proposed algorithm has only four distinct eigenvalues for any transform order whereas the FrFT has more than four distinct eigenvalues for non-integer orders.

Except for the work of Santhanam et al., the early work on DFrFT can mainly be split into two major groups. The first approach is based on the **S** matrix introduced by Dickinson

et al. [10], which is an almost-tridiagonal matrix commuting with the DFT matrix. As the **S** matrix commutes with the DFT matrix, they share at least one set of eigenvectors in common. Candan et al. used the second-order difference equation by approximating the second-order differential equation in which the homogenous solution set is the Hermite–Gauss functions [11]. Recently, Candan uses higher-order approximations to discrete derivative operator to approximate Hermite–Gauss functions better [12]. Instead, in [13] we suggest using infinite-order approximation to second derivative operator and find excellent Hermite–Gauss-like eigenvectors.

Pei et al. used the **S** matrix as a basis for obtaining a new basis, which is closer to the samples of Hermite–Gauss functions by employing Gram–Schmidt algorithm (GSA) and orthogonal Procrustes algorithm (OPA) [14]. Specifically, eigenvectors of the **S** matrix is projected onto the samples of the continuous Hermite–Gauss functions and GSA is employed to get eigenvectors, where the performance criteria is chosen as the norm of error between the discrete Hermite–Gauss-like vectors and the samples of the continuous Hermite–Gauss functions. OPA has been suggested as another technique, which is reasoned to minimize the Frobenius norm between the eigenvectors of the **S** matrix and the samples of the Hermite–Gauss functions. However, Hanna et al. show in

* Corresponding author. Tel.: +90 212 383 24 98;
fax: +90 212 383 24 86.

E-mail addresses: ahmet.serbes@gmail.com, aserbes@yildiz.edu.tr
(A. Serbes), lutfiye@ieee.org (L. Durak-Ata).

[18] that *any* matrix other than **S** could also be used as an initial matrix in this OPA and GSA methods without affecting the result.

The second approach is based on the tridiagonal **T** matrix defined by Grünbaum [15], which is later on refined by [16]. The **T** matrix is employed in combination with **S** matrix to furnish the basis of eigenvectors for the DFrFT matrix in [17] as **S**+k**T**, where k is an integer. Apart from these, Hanna et al. [18] have used the spectral theorem to decompose the ordinary-DFT matrix and obtained four projection matrices **P**$_i$ for i=1,2,3,4. The independent columns of **P**$_i$ are used as a basis for the DFrFT and this technique is called as **P** method. However, when used alone, the **P** method produces inaccurate results and the norm of error vector between the samples of continuous Hermite–Gauss functions and the orthogonal eigenvectors obtained by the **P** method are very high. To overcome inaccurate results, authors have employed OPA and sequential-OPA to minimize the error.

In this work, we focus on a different approach to derive eigenvectors of the DFT matrix in order to build the DFrFT matrix that mimics the properties of its continuous counterpart. A straightforward and refined derivation of the eigenvectors of the DFT matrix is proposed without using any commuting matrices, but using only the factored form of a basic property of the DFT matrix stating that four consecutive Fourier transforms is the identity transform, i.e.,

$$\mathbf{W}_N^4 = \mathbf{I}_N \tag{1}$$

where $\mathbf{W}_N$ and $\mathbf{I}_N$ are the centered DFT (CDFT) and the identity matrices of order N, respectively. We utilize factorization of the CDFT matrix to obtain new matrices, whose columns are eigenvectors of the CDFT matrix. We thereafter employ GSA to find the orthonormal eigenvectors obtained by factorization of the CDFT matrix. By employing a DFT-shift matrix **K**, eigenvectors of the ordinary-DFT matrix are obtained by using the CDFT matrix. We have also used the **S** and **T** matrices together with our method later on to boost the performance.

In [14], Pei et al. compute the samples of the Hermite–Gauss functions and employ GSA to orthogonalize these samples by projecting on the **S** matrix, which is equivalent to orthogonalizing the samples of the Hermite–Gauss functions without using the **S** matrix [18]. Hanna et al. claim to find the eigenvectors of the DFT matrix using a similar method to that of our work. However, they use the ordinary-DFT matrix as a basis to their work, but we employ the CDFT matrix. Additionally, they do not orthogonalize the non-orthogonal eigenvectors and they seem not to get eigenvectors similar to the samples of Hermite–Gauss functions. Our work is different from these works that we first find the non-orthogonal eigenvectors of the CDFT matrix without utilizing any **S** matrix or samples of the Hermite–Gauss functions and then we orthogonalize the obtained eigenvectors by employing the GSA. We do not use any samples of continuous Hermite–Gauss functions or project our proposed eigenvectors onto other matrices.

This paper is organized as follows. Section 2 gives introductory information on the FrFT and DFrFT. Sections 3 and 4 describe how to find the eigenvectors of the centered-DFrFT, the process to refine the eigenvectors to obtain a Hermite–Gaussian-like discrete eigenvector and to obtain the ordinary-DFrFT matrix. Section 5 compares the properties of the proposed method with the continuous FrFT. The performance of the proposed method is boosted in Section 6 and simulation results are given in Section 7. The paper concludes in Section 8.

2. Preliminaries

In this section, we define the continuous FrFT, give some of its properties, and present the underlying principals of the DFrFT.

2.1. Continuous FrFT

The a th-order continuous FrFT is defined as a linear unitary operator acting on an integrable function $f(u)$,

$$f_a(u) = \sqrt{1-\mathrm{j}\cot\alpha} \int_{-\infty}^{\infty} f(u)\exp(\mathrm{j}\pi(\cot\alpha u'^2 - 2\csc\alpha uu' + \cot\alpha u^2))\,\mathrm{d}u' \tag{2}$$

where $\alpha = a\pi/2$ is the transformation angle. The continuous FrFT kernel turns into the ordinary continuous Fourier transform (FT) kernel and inverse FT kernel for a=1 and 3, respectively. For a=4, the kernel is the identity operator and for a=2 it approaches to $\delta(u+u')$ in the limit. The FT has four distinct eigenvalues $\lambda \in \{1,-\mathrm{j},-1,\mathrm{j}\}$, since four consecutive FT is the identity transform. Hermite–Gauss functions are eigenfunctions of the FT satisfying

$$\mathcal{F}\{\psi_n(u)\} = e^{-\mathrm{j}n\pi/2}\psi_n(u) \tag{3}$$

where $\psi_n(u)$ is the n th-order Hermite–Gauss function associated with the eigenvalue $e^{-\mathrm{j}n\pi/2}$. The continuous FrFT satisfies the index additivity property [1]. From a signal processing prospect, one of the most important properties of the FrFT is its rotation property in time–frequency axis. FrFT rotates the time–frequency (or space–frequency) axis with an angle proportional to the transformation order a in counter-clockwise direction. An analogous statement of this property is that the FrFT rotates the signal in time–frequency axis of Wigner distribution with angle α in the clock-wise direction [1].

2.2. Centered-DFT and discrete FrFT

The N-point CDFT matrix $\mathbf{W}_N$ is defined as a unitary matrix whose elements are

$$(\mathbf{W}_N)_{n,m} = \frac{1}{\sqrt{N}}\exp\left(-\mathrm{j}\frac{2\pi}{N}(n-c)(m-c)\right),$$

$$n,m = 0,1,\ldots,N-1; \quad c = \frac{N-1}{2} \tag{4}$$

Let $\mathbf{I}_N$ be the identity matrix of order N, the CDFT matrix satisfies (1) and since four consecutive DFT operations correspond to the identity transform, the CDFT matrix has four distinct eigenvalues $\lambda \in \{1,-\mathrm{j},-1,\mathrm{j}\}$ as well. Using the eigenvalue decomposition, $\mathbf{W}_N$ can be written in

the form of

$$\mathbf{W}_N = \mathbf{U}_N \mathbf{\Lambda}_N \mathbf{U}_N^T \tag{5}$$

where $(\cdot)^T$ is the transpose operator, $\mathbf{U}$ is the real Hermite–Gauss-like eigenvectors of the CDFT matrix and $\mathbf{\Lambda}$ is the diagonal matrix containing the eigenvalues. As the continuous-time FrFT is a generalization of the FT with an order parameter a where $a \in [0, 4]$, we generalize the eigendecomposition-type FT expression into DFrFT by taking the ath fractional power of $\mathbf{W}_N$ matrix.

3. Eigenanalysis of the discrete fractional Fourier transform

The DFT maps the signal from $[0, N-1]$ discrete input space to $[0, 2\pi]$ discrete frequency space, whereas the CDFT maps $[-(N-1)/2, (N-1)/2]$ to $[-\pi, \pi]$. This allows CDFT to define even and odd-functions such as Hermite–Gauss functions, that is contrary to the ordinary DFT definition. In order to approximate the samples of the continuous FrFT and to imply the rotation property, Hermite–Gauss-like eigenvectors of the DFT matrix have to be obtained.

In this work, we use the CDFT matrix instead of the ordinary DFT matrix because the Hermite–Gauss-like vectors are eigenvectors of *only* the CDFT matrix, not the DFT matrix, i.e., when a discrete Hermite–Gauss-like eigenvector is transformed using the ordinary DFT matrix, the output is the shifted version of the Hermite–Gauss vector multiplied by a complex sinusoidal.

Proposition 1. *The Hermite–Gauss-like eigenvectors of the CDFT matrix are*

$$\mathbf{V}_1 = \frac{1}{2}(\mathbb{R}\{\mathbf{W}_N\} + (\mathbb{R}\{\mathbf{W}_N\})^2) \tag{6a}$$

$$\mathbf{V}_2 = -\frac{1}{2}(\mathbb{R}\{\mathbf{W}_N\} - (\mathbb{R}\{\mathbf{W}_N\})^2) \tag{6b}$$

$$\mathbf{V}_3 = \frac{1}{2}(\mathbb{I}\{\mathbf{W}_N\} + (\mathbb{I}\{\mathbf{W}_N\})^2) \tag{6c}$$

$$\mathbf{V}_4 = -\frac{1}{2}(\mathbb{I}\{\mathbf{W}_N\} - (\mathbb{I}\{\mathbf{W}_N\})^2) \tag{6d}$$

where columns of $\mathbf{V}_1$, $\mathbf{V}_2$, $\mathbf{V}_3$, and $\mathbf{V}_4$ are eigenvectors associated with the eigenvalues 1, -1, j, and $-j$, respectively. $\mathbb{R}$ and $\mathbb{I}$ denote the real and imaginary parts and $\mathbf{W}_N$ is the CDFT matrix as defined in (4).

Proof. Re-arranging (1) as $\mathbf{W}_N^4 - \mathbf{I}_N = 0$ and rewriting it in its factored form as

$$(\mathbf{W}_N - \mathbf{I}_N)(\mathbf{W}_N + \mathbf{I}_N)(\mathbf{W}_N - j\mathbf{I}_N)(\mathbf{W}_N + j\mathbf{I}_N) = 0_N \tag{7}$$

leads us to a very important result when rewritten in four different eigenequation forms for the DFT as stated earlier by Bose [19]. As for the eigenvectors associated with $\lambda = 1$, we obtain the eigenvalue problem

$$(\mathbf{W}_N - \mathbf{I}_N)(\mathbf{W}_N^3 + \mathbf{W}_N^2 + \mathbf{W}_N + \mathbf{I}_N) = 0_N \tag{8}$$

Hence, the eigenvector matrix whose columns *include* the eigenvectors is expressed by

$$\mathbf{V}_1 = (\mathbf{W}_N^3 + \mathbf{W}_N^2 + \mathbf{W}_N + \mathbf{I}_N) \tag{9a}$$

which satisfies $\mathbf{W}_N \mathbf{V}_1 = \mathbf{V}_1$ considering $\mathbf{W}_N^4 = I_N$. We note that some, but not all columns of $\mathbf{V}_1$ are linearly independent. The other matrices whose columns include eigenvectors of the CDFT matrix can be obtained in the same manner

$$\mathbf{V}_2 = (\mathbf{W}_N^3 - \mathbf{W}_N^2 + \mathbf{W}_N - \mathbf{I}_N) \tag{9b}$$

$$\mathbf{V}_3 = (\mathbf{W}_N^3 + j\mathbf{W}_N^2 - \mathbf{W}_N - j\mathbf{I}_N) \tag{9c}$$

$$\mathbf{V}_4 = (\mathbf{W}_N^3 - j\mathbf{W}_N^2 - \mathbf{W}_N + j\mathbf{I}_N) \tag{9d}$$

Obtained matrices are not full-rank and columns of these matrices are not linearly independent either, but their eigenvalues are of modulus 4, since $\mathbf{V}_1$, $\mathbf{V}_2$, $\mathbf{V}_3$, and $\mathbf{V}_4$ keep the eigenvectors with the associated eigenvalues only. Let us consider $\mathbf{V}_1 = \mathbf{W}_N^3 + \mathbf{W}_N^2 + \mathbf{W}_N + \mathbf{I}_N$ which can be expressed more explicitly as

$$\mathbf{V}_1 = \sum_{n=0}^{N-1} (e^{3(jn\pi/2)} + e^{2(jn\pi/2)} + e^{jn\pi/2} + 1)\mathbf{v}_n = \sum_{n=0}^{N-1} 4\mathbf{v}_{4n} \tag{10a}$$

since $\mathbf{W}_N = \sum_{n=0}^{N-1} e^{jn\pi/2}\mathbf{v}_n$, where $\mathbf{v}_n$ represents discrete Hermite Gaussian eigenvectors. Similarly using (9b)–(9d) $\mathbf{V}_2$, $\mathbf{V}_3$ and $\mathbf{V}_4$ are expressed as

$$\mathbf{V}_2 = \sum_{n=0}^{N-1} -4\mathbf{v}_{4n+2} \tag{10b}$$

$$\mathbf{V}_3 = \sum_{n=0}^{N-1} (4j)\mathbf{v}_{4n+3} \tag{10c}$$

$$\mathbf{V}_4 = \sum_{n=0}^{N-1} (-4j)\mathbf{v}_{4n+1} \tag{10d}$$

Consequently, columns of $\mathbf{V}_1$ keep *only* Hermite–Gauss-like eigenvectors of order $4n$ and analogously $\mathbf{V}_2$, $\mathbf{V}_3$ and $\mathbf{V}_4$ hold *only* Hermite-Gaussians of order $4n+2$, $4n+3$, and $4n+1$, respectively. Number of independent columns (or rank) corresponds to the multiplicities of the eigenvalues, shown in Table 1 [20]. Note that $\mathbf{V}_1$ and $\mathbf{V}_2$ are pure real and $\mathbf{V}_3$ and $\mathbf{V}_4$ are pure imaginary, since $\mathbf{W}_N^3 + \mathbf{W}_N$ and $\mathbf{W}_N^2$ are pure real and $\mathbf{W}_N^3 - \mathbf{W}_N$ is pure imaginary

$$\mathbf{W}_N^3 + \mathbf{W}_N = 2\mathbb{R}\{\mathbf{W}_N\} \tag{11a}$$

$$\mathbf{W}_N^3 - \mathbf{W}_N = -2j\mathbb{I}\{\mathbf{W}_N\} \tag{11b}$$

$$\mathbf{W}_N^2 + \mathbf{I}_N = 2(\mathbb{R}\{\mathbf{W}_N\})^2 \tag{11c}$$

$$\mathbf{W}_N^2 - \mathbf{I}_N = -2(\mathbb{I}\{\mathbf{W}_N\})^2 \tag{11d}$$

Table 1
Multiplicities of the eigenvalues of the $N \times N$ CDFT matrix.

N	λ			
	1	$-j$	-1	j
$4m$	m	m	m	m
$4m+1$	$m+1$	m	m	m
$4m+2$	$m+1$	$m+1$	m	m
$4m+3$	$m+1$	$m+1$	$m+1$	m

Substituting appropriate terms in (9) and (11), we obtain

$$\mathbf{V}_1 = 2(\mathbb{R}\{\mathbf{W}_N\} + (\mathbb{R}\{\mathbf{W}_N\})^2) \tag{12a}$$

$$\mathbf{V}_2 = 2(\mathbb{R}\{\mathbf{W}_N\} - (\mathbb{R}\{\mathbf{W}_N\})^2) \tag{12b}$$

$$\mathbf{V}_3 = -2\mathrm{j}(\mathbb{I}\{\mathbf{W}_N\} + (\mathbb{I}\{\mathbf{W}_N\})^2) \tag{12c}$$

$$\mathbf{V}_4 = -2\mathrm{j}(\mathbb{I}\{\mathbf{W}_N\} - (\mathbb{I}\{\mathbf{W}_N\})^2). \tag{12d}$$

Hermite–Gauss-like eigenvectors have to be real and unitary. In order to obtain real and unitary eigenvectors, we divide $\mathbf{V}_1$, $\mathbf{V}_2$, $\mathbf{V}_3$, and $\mathbf{V}_4$ by 4, -4, 4j and -4j, respectively, since these eigenvectors have eigenvalues of modulus 4. The proof is complete. □

Notice that all four $\mathbf{V}_i$ are commuting with the CDFT matrix and therefore have the eigenvectors divided into four multiplicities. However, since columns of these matrices are not linearly independent, they cannot be left in this form. The acquired eigenvectors that are columns of $\mathbf{V}_i$, for i=1–4 are employed in the calculation of the DFrFT matrix, which is discussed in the following section.

4. The DFrFT matrix

The FrFT operator of order a can be defined as the a th-power of the ordinary DFT operator $\mathbf{W}_N$. Hence, the DFrFT matrix can be expressed by means of its eigenvector decomposition,

$$\mathbf{W}_N^a = \mathbf{U}_N \mathbf{\Lambda}_N^a \mathbf{U}_N^T \tag{13}$$

where $\mathbf{\Lambda}_N^a$ is explicitly

$$\mathbf{\Lambda}_N^a = \mathrm{diag}(e^{-j0}, e^{-j\pi/2a}, \ldots, e^{-j\pi/2a(N-2)}, e^{-j\pi/2a(N-1)}) \tag{14}$$

for the centered-DFrFT [20].

As the columns of the matrices stated in (6) are not linearly independent (or full rank) an easy and quick way to obtain linearly independent and orthonormal columns of them is to

1. Compute the reduced echelon form of the matrices.
2. Pick *only* the columns associated with the pivots.
3. Employ an orthogonalization algorithm, e.g., Gram–Schmidt orthogonalization (GSO) algorithm.

We employ Gauss–Jordan elimination method to find the pivots and choose the linearly independent columns, therefore throw away some columns for each $\mathbf{V}_i$, for i = 1–4. Then, we employ the celebrated modified GSO (m-GSO) algorithm to obtain the normalized linearly independent orthonormal eigenvectors [21].

Recall that the reason of employing CDFT matrix is that, discrete Hermite–Gauss-like vectors are eigenvectors of the CDFT matrix, but the eigenvectors of DFT matrix are phase-shifted versions of the discrete Hermite–Gauss vectors. Applying the same method directly to the DFT matrix will produce incorrect results. Hanna et al. have derived similar equations to (9), however they have used the conventional DFT matrix and the spectral theorem and they have not obtained the linearly independent columns by utilizing an orthogonalization algorithm in [18]. The eigenvectors that

they have come up are completely different and consequently incorrect results are obtained.

4.1. Modified Gram–Schmidt algorithm

Despite the fact that the matrices stated in (6) are orthogonal to each other, columns of each individual matrix are neither linearly independent nor orthonormal. The Hermite–Gauss-like orthogonal CDFT eigenvectors can be obtained by employing the m-GSO. Let

- **y**: non-orthonormal columns of $\mathbf{V}_i$ after Gauss–Jordan elimination. (There are k_i columns for each $\mathbf{V}_i$.)
- $\overline{\mathbf{v}}$: orthonormal columns obtained by m-GSO.
- k_i: number of pivots in $\mathbf{V}_i$,

then for each $\mathbf{V}_i$ the algorithm is summarized in Algorithm 1. The m-GSO algorithm orthogonalizes any set of vectors by using projections and subtractions. As a first step, a vector is taken and the projections of the remaining vectors are subtracted from the vector, following a normalization step. The process is completed when this operation is carried out for all vectors.

Algorithm 1. The modified Gram–Schmidt algorithm.

```
for n = 1 to k_i do
    for m = 1 to n do
        y_n = y_n − (⟨y_m, y_n⟩ / ⟨y_m, y_m⟩) y_m
    end for
    v̄_n = y_n / ‖y_n‖
end for
```

4.2. The centered-DFrFT matrix

Let $\overline{\mathbf{V}}_i$, i=1,2,3,4 be the new linearly independent orthonormal eigenvector set after the m-GSO algorithm. The size of the $\overline{\mathbf{V}}_i$ matrix including the new eigenvectors is $N \times k_i$, where k_i is the rank of $\mathbf{V}_i$, which is already at hand after Gauss–Jordan elimination process. k_i can also be calculated by referring to the multiplicities of eigenvalues, which is shown in Table 1.

Obtaining the ordinary CDFT matrix: The ordinary CDFT matrix can be obtained by calculating the weighted sum of four eigenvalue decomposition of $\overline{\mathbf{V}}_i$ associated with the eigenvalues $\lambda = \{1, -1, \mathrm{j}, -\mathrm{j}\}$

$$\mathbf{W}_N = \overline{\mathbf{V}}_1 \mathbf{I}_{k_1} \overline{\mathbf{V}}_1^T + \overline{\mathbf{V}}_2 (-\mathbf{I}_{k_2}) \overline{\mathbf{V}}_2^T + \overline{\mathbf{V}}_3 (\mathrm{j}\mathbf{I}_{k_3}) \overline{\mathbf{V}}_3^T + \overline{\mathbf{V}}_4 (-\mathrm{j}\mathbf{I}_{k_4}) \overline{\mathbf{V}}_4^T \tag{15}$$

where $\mathbf{I}_{k_i}$ is the $k_i \times k_i$ identity matrix.

Sorting the eigenvectors: Sorting or indexing the eigenvectors is straightforward in this method. As we employ the CDFT matrix itself to obtain the eigenvectors, we come up with the sorted eigenvectors. There are n zero-crossings in a Hermite–Gauss function of order n. Since the zero-crossings in the CDFT matrix is sorted in descending order, i.e., there are no zero-crossings in the middle and there are $N-1$ zero crossings in the first column, the eigenvectors automatically appear in sorted order after the Gauss–Jordan elimination. That is, columns of all four $\overline{\mathbf{V}}_i$ contain

the highest order of discrete Hermite–Gauss-like eigenvector in its first column and the lowest order of discrete Hermite–Gauss-like eigenvector in its last column. For example, $\overline{\mathbf{V}}_1$ contain the zeroth-order Hermite–Gauss vector in its last column and $4(k_1-1)$-th order of Hermite–Gauss vector in its first column. The other columns in between are sorted in order of

$$\overline{\mathbf{V}}_1 = \begin{bmatrix} | & & | & | & | \\ \mathbf{h}_{4k_1-4} & \dots & \mathbf{h}_8 & \mathbf{h}_4 & \mathbf{h}_0 \\ | & & | & | & | \end{bmatrix} \tag{16a}$$

In a similar manner,

$$\overline{\mathbf{V}}_2 = \begin{bmatrix} | & & | & | & | \\ \mathbf{h}_{4k_2-2} & \dots & \mathbf{h}_{10} & \mathbf{h}_6 & \mathbf{h}_2 \\ | & & | & | & | \end{bmatrix} \tag{16b}$$

$$\overline{\mathbf{V}}_3 = \begin{bmatrix} | & & | & | & | \\ \mathbf{h}_{4k_3-1} & \dots & \mathbf{h}_{11} & \mathbf{h}_7 & \mathbf{h}_3 \\ | & & | & | & | \end{bmatrix} \tag{16c}$$

$$\overline{\mathbf{V}}_4 = \begin{bmatrix} | & & | & | & | \\ \mathbf{h}_{4k_4-3} & \dots & \mathbf{h}_9 & \mathbf{h}_5 & \mathbf{h}_1 \\ | & & | & | & | \end{bmatrix} \tag{16d}$$

are formed. Hence the associated eigenvalues $\lambda\mathbf{I}_{k_i}$ in (15) can be written explicitly for all λ

$$\mathbf{I}_{k_1} = \mathrm{diag}(e^{-j2\pi(k_1-1)},\dots,e^{-j2\pi},e^{-j0})$$

$$-\mathbf{I}_{k_2} = \mathrm{diag}(e^{-j(\pi+2\pi(k_2-1))},\dots,e^{-j3\pi},e^{-j\pi})$$

$$\mathbf{j}\mathbf{I}_{k_3} = \mathrm{diag}(e^{-j(3\pi/2+2\pi(k_3-1))},\dots,e^{-j7\pi/2},e^{-j3\pi/2})$$

$$-\mathbf{j}\mathbf{I}_{k_4} = \mathrm{diag}(e^{-j(\pi/2+2\pi(k_4-1))},\dots,e^{-j5\pi/2},e^{-j\pi/2}) \tag{17}$$

Obtaining the centered-DFrFT matrix: The centered-DFrFT matrix can be obtained by combining (13), (9) and (17) as

$$\mathbf{W}_N^a = \overline{\mathbf{V}}_1\overline{\mathbf{\Lambda}}_{k_1}^a\overline{\mathbf{V}}_1^T + \overline{\mathbf{V}}_2\overline{\mathbf{\Lambda}}_{k_2}^a\overline{\mathbf{V}}_2^T + \overline{\mathbf{V}}_3\overline{\mathbf{\Lambda}}_{k_3}^a\overline{\mathbf{V}}_3^T + \overline{\mathbf{V}}_4\overline{\mathbf{\Lambda}}_{k_4}^a\overline{\mathbf{V}}_4^T \tag{18}$$

where

$$\overline{\mathbf{\Lambda}}_{k_1}^a = \mathrm{diag}\left(e^{-j2\pi(k_1-1)a},\dots,e^{-j2\pi a},e^{-j0}\right) \tag{19a}$$

$$\overline{\mathbf{\Lambda}}_{k_2}^a = \mathrm{diag}\left(e^{-j(\pi+(k_2-1)2\pi)a},\dots,e^{-j3\pi a},e^{-j\pi a}\right) \tag{19b}$$

$$\overline{\mathbf{\Lambda}}_{k_3}^a = \mathrm{diag}\left(e^{-j(3\pi/2+(k_3-1)2\pi)a},\dots,e^{-j7\pi/2a},e^{-j3\pi/2a}\right) \tag{19c}$$

$$\overline{\mathbf{\Lambda}}_{k_4}^a = \mathrm{diag}\left(e^{-j(\pi/2+(k_4-1)2\pi)a},\dots,e^{-j5\pi/2a},e^{-j\pi/2a}\right) \tag{19d}$$

As $\overline{\mathbf{V}}_i$ are orthonormal to each other, (18) implies that the index additivity rule is supported:

$$\begin{aligned} \mathbf{W}_N^{a_1}\mathbf{W}_N^{a_2} &= (\overline{\mathbf{V}}_1\overline{\mathbf{\Lambda}}_{k_1}^{a_1}\overline{\mathbf{V}}_1^T + \overline{\mathbf{V}}_2\overline{\mathbf{\Lambda}}_{k_2}^{a_1}\overline{\mathbf{V}}_2^T + \overline{\mathbf{V}}_3\overline{\mathbf{\Lambda}}_{k_3}^{a_1}\overline{\mathbf{V}}_3^T \\ &\quad + \overline{\mathbf{V}}_4\overline{\mathbf{\Lambda}}_{k_4}^{a_1}\overline{\mathbf{V}}_4^T)(\overline{\mathbf{V}}_1\overline{\mathbf{\Lambda}}_{k_1}^{a_2}\overline{\mathbf{V}}_1^T + \overline{\mathbf{V}}_2\overline{\mathbf{\Lambda}}_{k_2}^{a_2}\overline{\mathbf{V}}_2^T + \overline{\mathbf{V}}_3\overline{\mathbf{\Lambda}}_{k_3}^{a_2}\overline{\mathbf{V}}_3^T \\ &\quad + \overline{\mathbf{V}}_4\overline{\mathbf{\Lambda}}_{k_4}^{a_2}\overline{\mathbf{V}}_4^T) = (\overline{\mathbf{V}}_1\overline{\mathbf{\Lambda}}_{k_1}^{a_1+a_2}\overline{\mathbf{V}}_1^T + \overline{\mathbf{V}}_2\overline{\mathbf{\Lambda}}_{k_2}^{a_1+a_2}\overline{\mathbf{V}}_2^T \\ &\quad + \overline{\mathbf{V}}_3\overline{\mathbf{\Lambda}}_{k_3}^{a_1+a_2}\overline{\mathbf{V}}_3^T + \overline{\mathbf{V}}_4\overline{\mathbf{\Lambda}}_{k_4}^{a_1+a_2}\overline{\mathbf{V}}_4^T) = \mathbf{W}_N^{a_1+a_2} \end{aligned} \tag{20}$$

In Section 5, the proposed method is tested whether the proposed centered-DFrFT approximates the samples of its continuous counterpart.

4.3. Obtaining the DFrFT matrix

There is a close relationship between the CDFT and ordinary-DFT matrices; they can be transformed to each other in some circumstances. The only difference between the CDFT and the ordinary-DFT is the offset in the location of the signal. The transform domain signal by the ordinary-DFT is the *shifted* version of the CDFT-domain signal. When CDFT of an odd-length signal is taken and the left and right halves of the signal is swapped, the ordinary-DFT-domain of the signal is obtained. We call this operation the *DFT-shift*.[1]

Let $\mathbf{W}_N$ and $\mathbf{F}_N$ be the $N \times N$ CDFT and ordinary-DFT matrices, respectively. We analyze the relationship between them for N odd and even separately. For odd N, $\mathbf{F}_N$ is related with $\mathbf{W}_N$ through the permutation matrix $\mathbf{K}_N$ as

$$\mathbf{F}_N = \mathbf{K}_N\mathbf{W}_N\mathbf{K}_N^{-1} \tag{21}$$

where the DFT-shift permutation matrix $\mathbf{K}_N$ can be written by

$$\mathbf{K}_N = \begin{bmatrix} \mathbf{0} & \mathbf{I}_k \\ \mathbf{I}_{N-k} & \mathbf{0} \end{bmatrix} \tag{22}$$

where $\mathbf{I}_k$ and $\mathbf{I}_{N-k}$ are $k \times k$ and $(N-k) \times (N-k)$ identity matrices and $k=(N+1)/2$.

In this case, the permutation matrix is equal to its inverse, i.e., $\mathbf{K}_N = \mathbf{K}_N^{-1}$. Eq. (21) is reduced to $\mathbf{F}_N = \mathbf{K}_N\mathbf{W}_N\mathbf{K}_N$. Therefore, $\mathbf{F}_N$ and $\mathbf{W}_N$ are similar matrices. Hence, their eigenvalues are the same and their eigenvectors are related through $\mathbf{K}_N$ matrix. $\mathbf{K}_N$ swaps left and right halves of the signal.

The discrete Hermite–Gauss vectors are not eigenvectors of the ordinary-DFT matrix, since they are eigenvectors of the CDFT matrix. Let $\mathbf{h}_n$ be the n th-order discrete Hermite–Gauss-like vector, the ordinary-DFT transform satisfies

$$\mathbf{F}_N\mathbf{K}_N\mathbf{h}_n = \lambda_n\mathbf{K}_N\mathbf{h}_n \tag{23}$$

as the eigenvectors of the ordinary-DFT transform is circularly shifted versions of the Hermite-Gaussians. Here, λ_n is the eigenvalue associated with the eigenvector $\mathbf{h}_n$.

For N even, we have to define $\mathbf{W}_N$ in a different way as $c = N/2+1$ in (4), to satisfy (23). $\mathbf{K}_N$ in (22) is modified to

$$\mathbf{K}_N = \begin{bmatrix} \mathbf{0} & \mathbf{I}_{N/2} \\ \mathbf{I}_{N/2} & \mathbf{0} \end{bmatrix} \tag{24}$$

where $\mathbf{I}_{N/2}$ is an $N/2 \times N/2$ identity matrix. When the CDFT matrix is defined accordingly, multiplicities of the eigenvalues change. However, new multiplicities of eigenvalues are exactly the same as the ordinary-DFT matrix and computations have to be done by taking them into consideration (see Table 2). A comparison of Tables 1 and 2 shows that the multiplicities of eigenvalues remain

---

[1] This operation is also valid as a function named *fftshift*(...) in MATLAB®.

Table 2
Multiplicities of the eigenvalues of the $N \times N$ ordinary DFT matrix.

N	λ			
	1	$-j$	-1	j
$4m$	$m+1$	m	m	$m-1$
$4m+1$	$m+1$	m	m	m
$4m+2$	$m+1$	m	$m+1$	m
$4m+3$	$m+1$	$m+1$	$m+1$	m

the same for odd N, while it is different for even N. Eq. (19) is modified into $\Lambda_N^a = \text{diag}(e^{-j0}, e^{-j(\pi/2)a}, \ldots, e^{-j(\pi/2)a(N-2)}, e^{-j(\pi/2)aN})$ by making a *by-pass* in the last eigenvalue. Hence, for $N=4m+2$ we only change (19b) to

$$\overline{\Lambda}_{k_2}^a = \text{diag}(e^{-j(\pi+k_2 2\pi)a}, e^{-j(\pi+(k_2-2)2\pi)a}, \ldots, e^{-j3\pi a}, e^{-j\pi a}) \tag{25a}$$

and for $N=4m$ it is sufficient that *only* (19c) is changed to

$$\overline{\Lambda}_{k_4}^a = \text{diag}(e^{-j(\pi/2+k_4 2\pi)a}, e^{-j(\pi/2+(k_4-2)2\pi)a}, \ldots, e^{-j5\pi/2 a}, e^{-j\pi/2 a}) \tag{25b}$$

Eq. (21) also holds for even N. To sum up, the ordinary-DFrFT with order a can be expressed by

$$\mathbf{F}_N^a = \mathbf{K}_N \mathbf{W}_N^a \mathbf{K}_N^{-1} \tag{26}$$

The acquired eigenvectors $\overline{V}_i$, for i = 1–4 are employed in the calculation of the DFrFT matrix, which is discussed in the following section.

5. Numerical verification of the proposed $\overline{V}$ method

The proposed $\overline{V}$ method satisfies unitarity and angle additivity properties. In parallel to the continuous FrFT [1], it reduces to the ordinary DFT when a = 1 and it approximates to the samples of the continuous FrFT for fractional values of a. To numerically verify, we have transformed a discrete square-wave signal $\mathbf{x}[n]$ of length $N=73$

$$\mathbf{x}[n] = \begin{cases} 1 & \text{if } -6 \leq n \leq 6 \\ 0 & \text{otherwise} \end{cases} \tag{27}$$

Fig. 1 shows DFrFRT of the rectangular function of various transform orders and Fig. 2 shows the samples of the continuous FrFT of $x[n]$ for the same transform orders. As it is clear from the figures, the proposed method approximates the samples of its continuous counterpart. Table 3 shows the normalized error between the samples of the signal using continuous FrFT and the proposed DFrFT in which the error is defined as

$$\text{Error} = \frac{\|\mathbf{x}_a - \overline{\mathbf{x}}_a\|}{\|\mathbf{x}\|} \tag{28}$$

where $\| \cdot \|$ is the norm operator, $\mathbf{x}_a$ and $\overline{\mathbf{x}}_a$ are the samples of continuous FrFT and the proposed DFrFT of the signal $\mathbf{x}$ of order a. Table 3 also gives a comparison of the normalized errors when the $\mathbf{S}$, $(\mathbf{S}+15\mathbf{T})$ as in [17], and new $(\mathbf{S}+30\mathbf{T}-7\mathbf{V}_T)$ methods are utilized. A detailed presentation and discussion of $(\mathbf{S}+30\mathbf{T}-7\mathbf{V}_T)$ method is given in Section 6. The derivations of both $\mathbf{S}$ and $\mathbf{T}$ matrices are given in Appendices A and B, respectively.

6. Boosting the performance

Performance of the proposed algorithm can be improved by using it in combination with $\mathbf{S}$ and $\mathbf{T}$ matrices. Pei et al. [17] uses the $\mathbf{S}$ method together with the Grünbaum's $\mathbf{T}$ matrix as a linear combination, in which it has been observed that Hermite–Gauss-like eigenvectors of $(\mathbf{S}+15\mathbf{T})$ are more accurate than both $\mathbf{S}$ and $\mathbf{T}$ alone.

In this section we suggest determining eigenvectors of linear combinations of $\mathbf{S}$, $\mathbf{T}$, $\mathbf{V}_T$ matrices to improve the performance by defining a new commuting matrix

$$\mathbf{V_T} = \overline{\mathbf{V}}_N \Lambda_{\mathbf{T}} \overline{\mathbf{V}}_N^T \tag{29}$$

where $\overline{\mathbf{V}}_N$ is the $N \times N$ sorted eigenvectors in the ascending order of zero-crossings obtained by the proposed method. $\Lambda_{\mathbf{T}}$ contains sorted eigenvalues of the $\mathbf{T}$ matrix in its diagonal, and $(\cdot)^T$ is the transpose operator.

Proposition. $\mathbf{V_T}$ commutes with the DFT matrix, i.e., $\mathbf{V_T W}_N = \mathbf{W}_N \mathbf{V_T}$.

Proof. As the columns of $\overline{\mathbf{V}}_N$ are eigenvectors of the DFT matrix, then the DFT matrix can be written as

$$\mathbf{W}_N = \mathbf{V}_N \Lambda_{\mathbf{W}} \mathbf{V}_N^T \tag{30}$$

where $\Lambda_{\mathbf{W}}$ is the diagonal matrix containing the eigenvalues of the DFT matrix. $\mathbf{V_T W}_N$ can be expressed as

$$\begin{aligned} \mathbf{V_T W}_N &= \mathbf{V}_N \Lambda_{\mathbf{T}} \mathbf{V}_N^T \mathbf{V}_N \Lambda_{\mathbf{W}} \mathbf{V}_N^T = \mathbf{V}_N \Lambda_{\mathbf{T}} \Lambda_{\mathbf{W}} \mathbf{V}_N^T = \mathbf{V}_N \Lambda_{\mathbf{W}} \Lambda_{\mathbf{T}} \mathbf{V}_N^T \\ &= \mathbf{V}_N \Lambda_{\mathbf{W}} \mathbf{V}_N^T \mathbf{V}_N \Lambda_{\mathbf{T}} \mathbf{V}_N^T = \mathbf{W}_N \mathbf{V_T} \end{aligned} \tag{31}$$

which concludes the proof. □

$\mathbf{T}$ matrix is tridiagonal and has discrete Hermite–Gauss-like eigenvectors similar to the proposed eigenvectors. Since we interchange eigenvectors of the $\mathbf{T}$ matrix with our proposed eigenvectors, the output $\mathbf{V_T}$ will be similar to the $\mathbf{T}$ matrix. The $\mathbf{V_T}$ is found to be nearly tridiagonal with large-magnitude values on three of its diagonals and small values on the others.

We propose that eigenvectors of linear combinations of $\mathbf{S}$, $\mathbf{T}$, and $\mathbf{V_T}$ matrices as $k_1\mathbf{S}+k_2\mathbf{T}+k_3\mathbf{V_T}$ produce more accurate eigenvectors. Performance criteria is chosen as norms of error between the samples of continuous Hermite–Gauss functions and the discrete Hermite–Gauss-like eigenvectors.

We have done computer experiments based on genetic algorithms and pattern search and found out that when k_1 = 1, k_2 = 30, and k_3 = -7 total norm of error is approximately minimum. Computation of the eigenvectors of the proposed $\mathbf{S}+30\mathbf{T}-7\mathbf{V_T}$ method can be done similar to [17].

Pei et al. showed that using the linear combination of $\mathbf{S}$ and $\mathbf{T}$ as $\mathbf{S}+15\mathbf{T}$ produces better results than the $\mathbf{S}$ or $\mathbf{T}$ alone. We also show that using $\mathbf{S}+30\mathbf{T}-7\mathbf{V}_T$ produces a more accurate approximation to the continuous FrFT. Using (28) as a measure of error, Table 3 shows comparison of the error for a square function. The results show that $\mathbf{S}+30\mathbf{T}-7\mathbf{V}_T$ approximate the continuous FrFT better than $\mathbf{S}$, $\overline{\mathbf{V}}$, or $\mathbf{S}+15\mathbf{T}$. Comparative presentation of performances of the proposed methods are shown in the following section in detail.
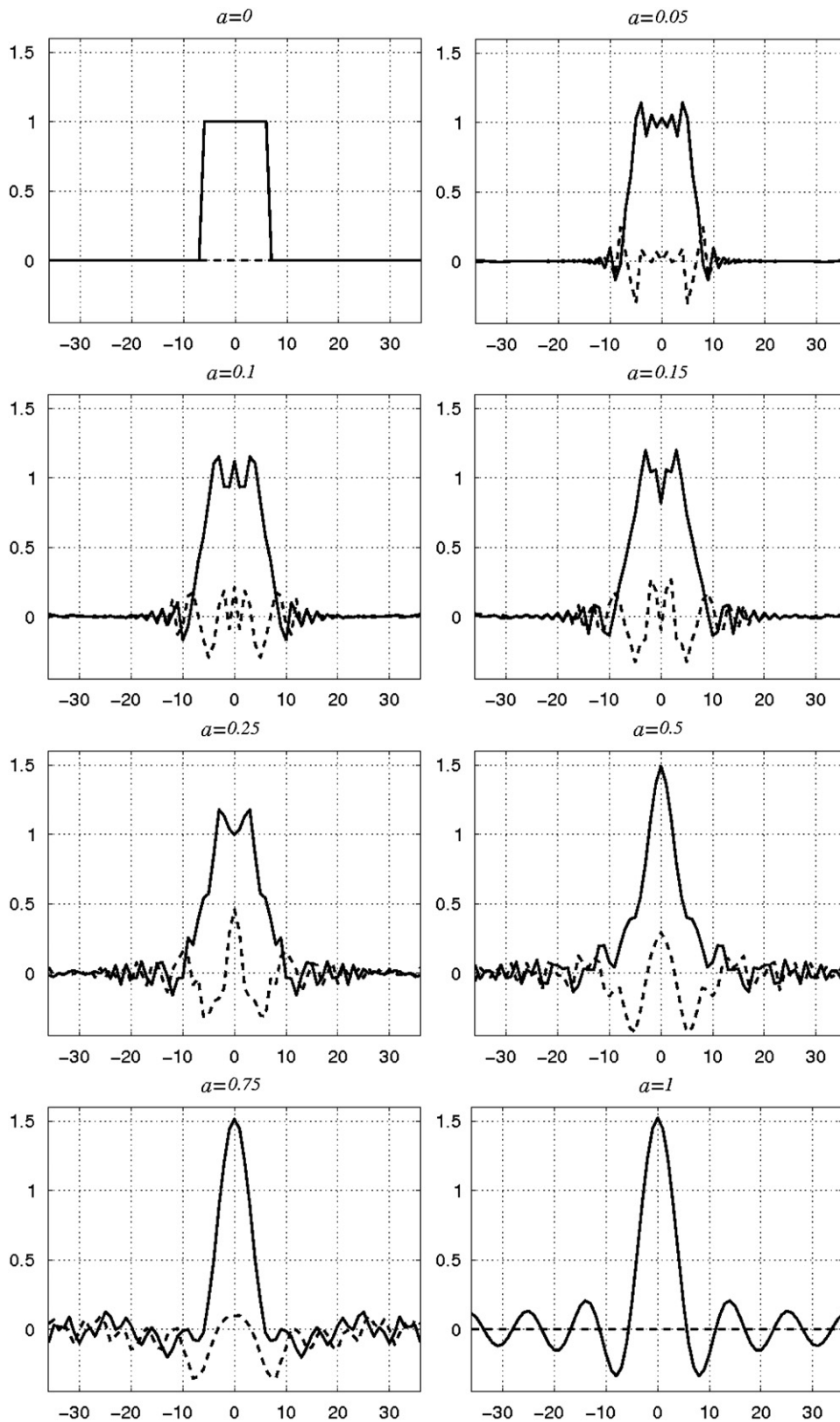
Fig. 1. DFrFT of a discrete rectangular function by the proposed method at various transform orders. Solid: real part, dashed: imaginary part.
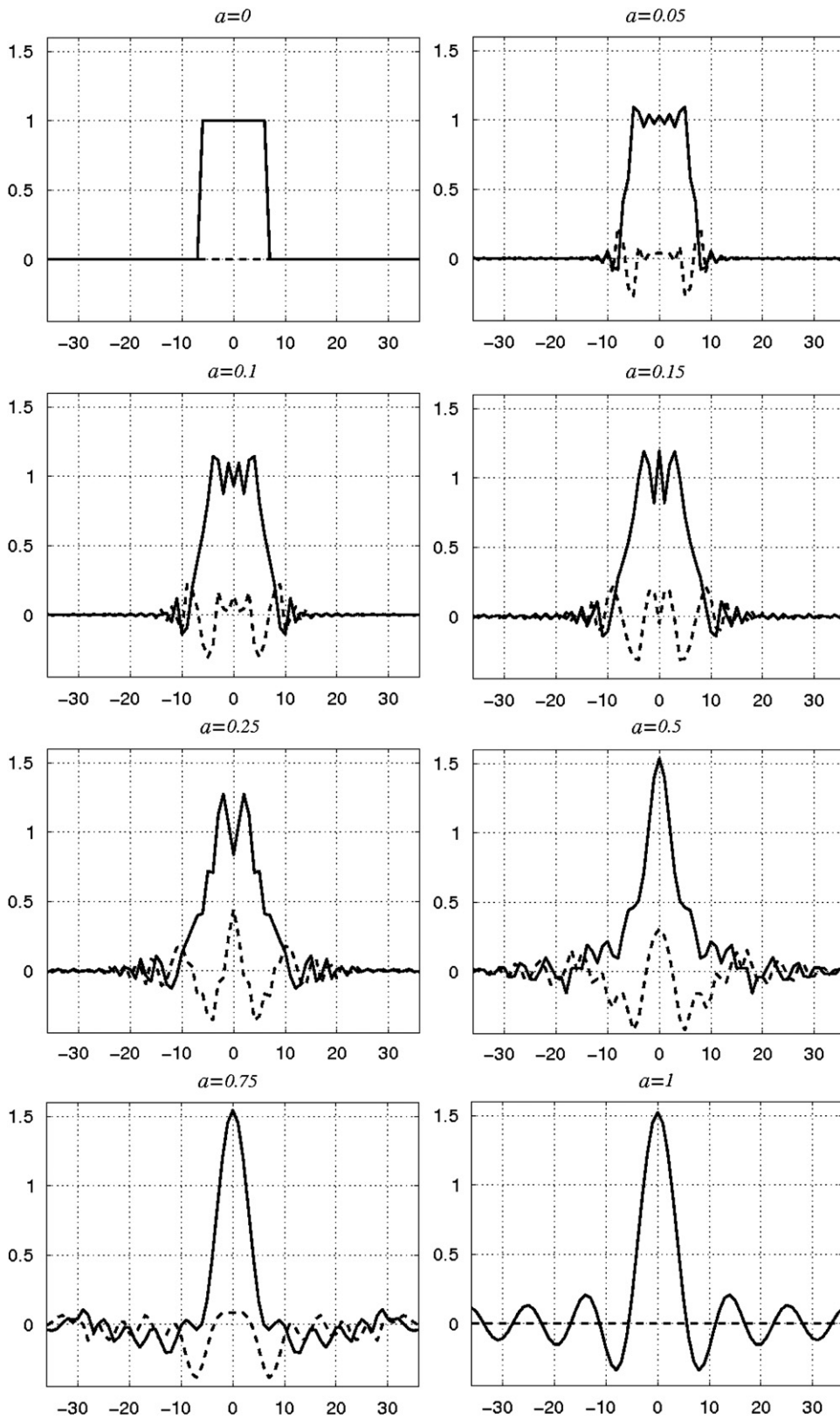
Fig. 2. Samples of the continuous FrFT of the rectangular function at various transform orders. Solid: real part, dashed: imaginary part.

Table 3
Normalized error between the continuous FrFT and the DFrFTs for the signal and orders given in Fig. 1.

a	Error			
	$\overline{\mathbf{V}}$	$\mathbf{S}$	$\mathbf{S}+15\mathbf{T}$	$\mathbf{S}+15\mathbf{T}-7\mathbf{V}_T$
0.05	0.0829	0.0612	0.0181	0.0160
0.10	0.1481	0.1155	0.0282	0.0193
0.15	0.1866	0.1524	0.0535	0.0412
0.25	0.2017	0.1538	0.0686	0.0482
0.50	0.3156	0.2038	0.0764	0.0541
0.75	0.2048	0.1567	0.0625	0.0437
1.00	0.0000	0.0000	0.0000	0.0000
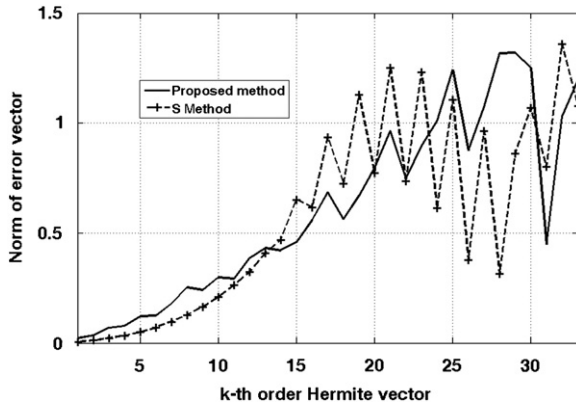
Fig. 3. Error norms of the discrete Hermite–Gauss like eigenvectors for the proposed method ($\overline{\mathbf{V}}$ method) and the $\mathbf{S}$ matrix approach for $N=33$.

7. Simulations

We have proposed two techniques for DFrFT.

1. First method is the $\overline{\mathbf{V}}$ method, where $\overline{\mathbf{V}}$ is the m-GSA output of (6) as discussed in Section 3.
2. The second method depends on $\mathbf{S}+30\mathbf{T}-7\mathbf{V_T}$ matrix, as presented in Section 6.

Fig. 3 shows the performance of the proposed method in which the norm of error vectors between the samples of continuous Hermite–Gauss functions and the orthonormal eigenvectors are chosen as the performance criteria. The performance of the proposed $\overline{\mathbf{V}}$ method is compared to the performance of the $\mathbf{S}$ method [11] for $N=33$. Even though the $\mathbf{S}$ method performs better for small orders, the $\overline{\mathbf{V}}$ method is better for middle-orders. Comparison of the $\mathbf{S}$ method and $\overline{\mathbf{V}}$ method for $N=65$ is shown in Fig. 4.

Norms of error vectors between the samples of the continuous Hermite–Gauss functions and the eigenvectors of the $\mathbf{S}+15\mathbf{T}$ method [17] and the eigenvectors of the proposed ($\mathbf{S}+30\mathbf{T}-7\mathbf{V_T}$) method for $N=33$ are compared in Fig. 5. It is clear that the proposed ($\mathbf{S}+30\mathbf{T}-7\mathbf{V_T}$) method outperforms compared to the $\mathbf{S}+15\mathbf{T}$ method.
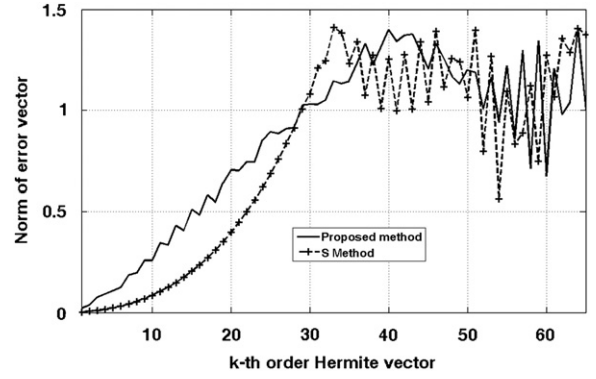
Fig. 4. Error norms of the discrete Hermite–Gauss like eigenvectors for the proposed method ($\overline{\mathbf{V}}$ method) and the $\mathbf{S}$ matrix approach for $N=65$.
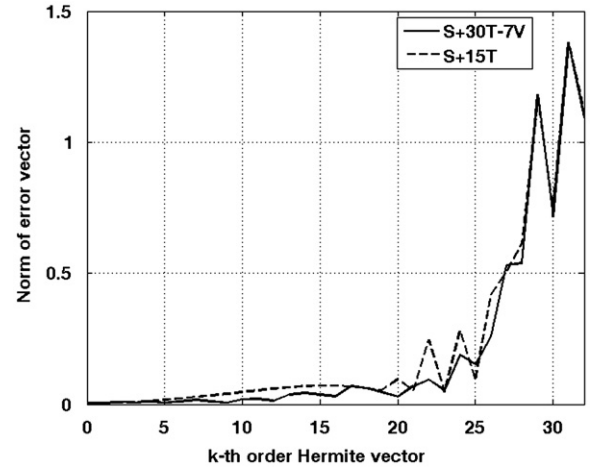
Fig. 5. Error norms of the discrete Hermite–Gauss like eigenvectors for the $\mathbf{S}+15\mathbf{T}-7\mathbf{V_T}$ method and $\mathbf{S}+15\mathbf{T}$ matrix approach for $N=33$.
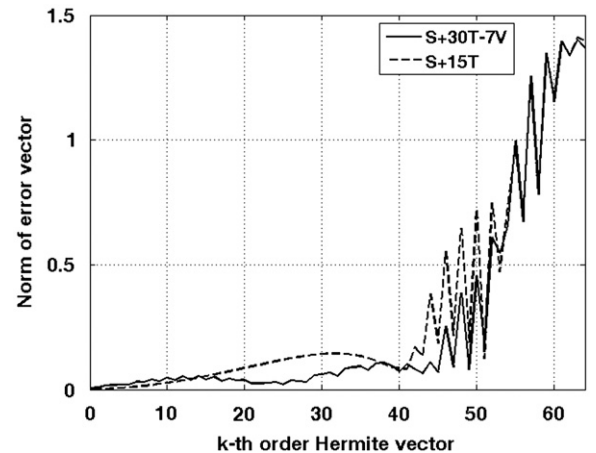
Fig. 6. Error norms of the discrete Hermite–Gauss like eigenvectors for the $\mathbf{S}+15\mathbf{T}-7\mathbf{V_T}$ method and $\mathbf{S}+15\mathbf{T}$ matrix approach for $N=65$.

Comparison of the **S**+15**T** and (**S**+30**T**−7**V_T**) approaches for $N=65$ is shown in Fig. 6. The latter approach with **V_T** outperforms the former in terms of the error norm.

8. Conclusions

In this work, we introduce a new way of obtaining an approximation to DFrFT matrix based on the idea that four consecutive Fourier transforms of a signal returns the signal itself. We employ a simple and elegant procedure to establish the eigenvectors of CDFT matrix by using only the CDFT matrix itself and its powers. After obtaining the new set of eigenvectors of the CDFT matrix, we present a straightforward way to transform the centered-DFrFT matrix into the ordinary DFrFT matrix. The simulation results show that the proposed method outperforms the **S** method for some orders.

To obtain a better set of Hermite–Gauss-like discrete eigenvectors, we generate a new commuting matrix **V_T** and appropriately combine it with the other commuting matrices **S** and **T**. Computer experiments show that the new commuting matrix (**S**+30**T**−7**V_T**) generates closer samples to the samples of Hermite–Gauss functions than developed before.

Acknowledgment

Appendix A. The S matrix

The **S**-matrix approach is a discrete solution to the second-order Hermite–Gauss-generating differential equation [11]

$$\frac{d^2}{dt^2}h(t)-4\pi t^2 h(t)=\lambda h(t) \tag{A.1}$$

where $h(t)$ is a continuous Hermite–Gauss function. Using Euler's formula for the differentiation

$$\frac{d^2}{dt^2}h(t)\approx\frac{h(n+\delta)-2h(n)+h(n-\delta)}{\delta^2} \tag{A.2}$$

where $\delta=1/\sqrt{N}$. In order to obtain a linear transformation matrix, the Taylor expansion

$$\cos\theta=1-\frac{\theta^2}{2}+O(\theta^4) \tag{A.3}$$

is used as $\theta^2\approx 2(1-\cos\theta)$. After appropriate substitutions using $t=n\delta$

$$h(n+1)-2h(n)+h(n-1)+2\left(\cos\left(\frac{2\pi n}{N}\right)-1\right)h(n)=\lambda h(n) \tag{A.4}$$

is obtained. Consequently the **S** matrix can be expressed as

$$\mathbf{S}=\begin{bmatrix} -2 & 1 & 0 & \dots & 0 & 1 \\ 1 & 2\cos\left(\frac{2\pi}{N}\right)-4 & 1 & \dots & 0 & 0 \\ 0 & 1 & 2\cos\left(\frac{2\pi}{N}2\right)-4 & \dots & 0 & 0 \\ \vdots & \vdots & \vdots & \ddots & \vdots & \vdots \\ 1 & 0 & 0 & \dots & 1 & 2\cos\left(\frac{2\pi}{N}(N-1)\right)-4 \end{bmatrix} \tag{A.5}$$

The **S** matrix commutes with the ordinary DFT matrix and therefore they share at least one set of common eigenvectors. To obtain the set of eigenvectors commuting with the centered case we have to transform it by using the **T**-matrix given in Section 4.3. Consider a centered discrete Hermite–Gauss-like vector,

$$\mathbf{SK}h(n)=\mathbf{K}h(n) \tag{A.6}$$

where **K** is defined in (22). To obtain the centered **S** matrix, both sides are multiplied with $\mathbf{K}^{-1}$,

$$(\mathbf{K}^{-1}\mathbf{SK})h(n)=h(n) \tag{A.7}$$

Consequently, the centered version of the **S** matrix can be obtained by $\mathbf{K}^{-1}\mathbf{SK}$.

Appendix B. The T matrix

The **T** matrix is defined as in (B.1). The derivation of this matrix is inspired from the work of Grünbaum [15] and is explained in [17] in detail. The **S** matrix chooses $\delta=1/\sqrt{N}$ as a sampling rate. However in the derivation of **T** matrix a smaller sampling rate $\delta=1/3\sqrt{N}$ is chosen as a sampling rate to approximate the second-order differential equation in (A.1) better. After appropriate calculations and approximations

$$\mathbf{T}=\begin{bmatrix} 1 & 0.5 & 0 & \dots & 0 & 0.5 \\ 0.5 & \left(\cos\left(\frac{\pi}{N}\right)\right)^2 & \frac{\cos\frac{\pi}{N}\cos\frac{2\pi}{N}}{2\cos(\pi/N)} & \dots & 0 & 0 \\ 0 & \frac{\cos\frac{\pi}{N}\cos\frac{2\pi}{N}}{2\cos(\pi/N)} & \left(\cos\left(\frac{2\pi}{N}\right)\right)^2 & \dots & 0 & 0 \\ \vdots & \vdots & \vdots & \ddots & \vdots & \vdots \\ 0.5 & 0 & 0 & \dots & \frac{\cos\frac{(N-2)\pi}{N}\cos\frac{(N-1)\pi}{N}}{2\cos(\pi/N)} & \left(\cos\left(\frac{(N-1)\pi}{N}\right)\right)^2 \end{bmatrix} \tag{B.1}$$

$$\frac{\cos\frac{(n-1)\pi}{N}\cos\frac{n\pi}{N}}{\cos(\pi/N)}h(n-1)+\left[2\cos\left(\frac{n\pi}{N}-4\right)\right]h(n)$$

$$+\frac{\frac{\cos n\pi}{N}\frac{\cos(n+1)\pi}{N}}{\cos(\pi/N)}h(n+1)=(2\lambda-4)h(n) \qquad (B.2)$$

is obtained which produces the **T** matrix. The centered version of the **T** matrix can be obtained similar to (A.7) as $\mathbf{K}^{-1}\mathbf{TK}$.

References

[1] H.M. Ozaktas, Z. Zalevski, M.A. Kutay, The Fractional Fourier Transform with Applications in Optics and Signal Processing, Wiley and Sons, New York, 2001.

[2] L. Durak, Time–Frequency Analysis: Novel Techniques for Deterministic Signals, VDM Verlag, Germany, 2009.

[3] L. Durak, O. Arikan, Short-time Fourier transform: two fundamental properties and an optimal implementation, IEEE Trans. Signal Process. 51 (5) (May 2003) 1231–1242.

[4] S.N. Sharma, R. Saxena, S.C. Saxena, Tuning of FIR filter transition bandwidth using fractional Fourier transform, Signal Process. 80 (8) (December 2007) 1501–1513.

[5] C. Vijaya, J.S. Bhat, Signal compression using discrete fractional Fourier transform and set partitioning in hierarchical tree, Signal Process. 86 (8) (August 2006) 1976–1983.

[6] K.K. Sharma, S.D. Joshi, Time delay estimation using fractional Fourier transform, Signal Process. 87 (5) (May 2007) 853–865.

[7] P.J. Oonincx, Joint time–frequency offset detection using the fractional Fourier transform, Signal Process. 88 (12) (December 2008) 2936–2942.

[8] D. Mendlovic, H.M. Ozaktas, A.W. Lohmann, Fractional correlation, Appl. Opt. 34 (1995) 303–309.

[9] B. Santhanam, J.H. McClellan, The discrete rotational Fourier transform, IEEE Trans. Signal Process. 44 (4) (April 1996) 994–998.

[10] B.W. Dickinson, K. Steiglitz, Eigenvalues and eigenvectors of the discrete Fourier transform, IEEE Trans. Acoust. Speech Signal Process. 30 (1) (February 1982) 25–31.

[11] C. Candan, M.A. Kutay, H.M. Ozaktas, The discrete fractional Fourier transform, IEEE Trans. Signal Process. 48 (5) (May 2000) 1329–1337.

[12] C. Candan, On higher order approximations for Hermite-Gaussian functions and discrete fractional Fourier transforms, IEEE Signal Process. Lett. 14 (10) (October 2007) 699–702.

[13] A. Serbes, L. Durak-Ata, Efficient computation of DFT commuting matrices by a closed-form infinite order approximation to the second differentiation matrix, Signal Process., this issue, doi:10.1016/j.sigpro.2010.05.002.

[14] S.C. Pei, M.H. Yeh, C.C. Tseng, Discrete fractional Fourier transform based on orthogonal projections, IEEE Trans. Signal Process. 47 (5) (May 1999) 1335–1348.

[15] F.A. Grünbaum, The eigenvectors of the discrete Fourier transform: A version of the Hermite functions, J. Math. Anal. Appl. 88 (2) (1982) 355–363.

[16] D.H. Mugler, S. Clary, Discrete hermite functions and the fractional Fourier transform, in: Proc. International Conference on Sampling Theory Application, Orlando, FL, 2001, pp. 303–308.

[17] S.C. Pei, V.L. Hsue, J.J. Ding, Discrete fractional Fourier transform based on new nearly tridiagonal commuting matrices, IEEE Trans. Signal Process. 54 (10) (October 2006) 3815–3828.

[18] M.T. Hanna, N.P.A. Seif, W.A.E.M. Ahmed, Hermite-Gaussian-like eigenvectors of the discrete Fourier transform matrix based on the singular-value decomposition of its orthogonal projection matrices, IEEE Trans. Circ. Syst. I: Regular Papers 51 (11) (November 2006) 2245–2254.

[19] N.K. Bose, Eigenvectors and eigenvalues of 1-D and n-D DFT matrices, AEÜ Int. J. Electron. Commun. 55 (2) (2001) 131–133.

[20] J.G. Vargas-Rubio, B. Santhanam, On the multiangle centered discrete fractional Fourier transform, IEEE Signal Process. Lett. 12 (4) (April 2005) 273–276.

[21] G.H. Golub, C.F. Van Loan, Matrix Computations, third ed., Johns Hopkins University Press, London, 1996.